

Manuscript Details

Manuscript number	EFA_2018_1314_R2
Title	Rail Accident Analysis using Large-Scale Investigations of Train Derailments on Switches and Crossings : Comparing the Performances of A Novel Stochastic Mathematical Prediction and Various Assumptions
Article type	Research Paper

Abstract

Each day tens of turnout-related derailment occur across the world. Not only is the prediction of them quite complex and difficult, but this also requires a comprehensive range of applications, and managing a well-designed geographic information system. With the advent of Geographic Information Systems (GIS), and computers-aided solutions, the last two decades have witnessed considerable advances in the field of derailment prediction. Mathematical models with many assumptions and simulations based on fixed algorithms were also introduced to estimate derailment rates. While the former requires a costly investment of time and energy to try and find the most fitting mathematical solution, the latter is sometimes a high hurdle for analysts since the availability and accessibility of geospatial data are limited, in general. As train safety and risk analysis rely on accurate assessment of derailment likelihood, a guide for transportation research is needed to show how each technique can approximate the number of observed derailments. In this study, a new stochastic mathematical prediction model has been established on the basis of a hierarchical Bayesian model (HBM), which can better address unique exposure indicators in segmented large-scale regions. Integration of multiple specialized packages, namely, MATLAB for image processing, R for statistical analysis, and ArcGIS for displaying and manipulating geospatial data, are adopted to unleash complex solutions that will practically benefit the rail industry and transportation researchers.

Keywords Derailment, Turnout component failures, Hierarchical Bayesian analysis, Freight transportation, Spatial analysis

Order of Authors SERDAR DINDAR, Sakdirat Kaewunruen, Min An

Submission Files Included in this PDF

File Name [File Type]

highlights.docx [Highlights]

manuscript.docx [Manuscript File]

To view all the submission files, including those not included in the PDF, click on the manuscript title on your EVISE Homepage, then click 'Download zip file'.

Research Data Related to this Submission

Engineering Failure Analysis

- 1 • All estimates seem to be incapable of calculating an estimate for a low number of derailments.
- 2 • It is determined that it is possible for a precise estimate of the derailment rates to be determined
- 3 under any uncertainty, which might be formed by the assumptions.
- 4 • Some assumptions which relied on turnout counts, are observed to deviate from the
- 5 observations
- 6 • It can be identified that the assumptions regarding turnout counts are a weak spot even when
- 7 being generated mathematically on the basis of a concrete belief.

1 **Rail Accident Analysis using Large-Scale Investigations of Train**
2 **Derailments on Switches and Crossings: Comparing the Performances**
3 **of a Novel Stochastic Mathematical Prediction and Various**
4 **Assumptions**

5

6 Keywords: Derailment, Turnout component failures, Hierarchical Bayesian analysis, Freight
7 transportation, Spatial analysis

8 **1 ABSTRACT**

9 Each day tens of turnout-related derailment occur across the world. Not only is the prediction of them
10 quite complex and difficult, but this also requires a comprehensive range of applications, and
11 managing a well-designed geographic information system. With the advent of Geographic
12 Information Systems (GIS), and computers-aided solutions, the last two decades have witnessed
13 considerable advances in the field of derailment prediction. Mathematical models with many
14 assumptions and simulations based on fixed algorithms were also introduced to estimate derailment
15 rates. While the former requires a costly investment of time and energy to try and find the most
16 fitting mathematical solution, the latter is sometimes a high hurdle for analysts since the availability
17 and accessibility of geospatial data are limited, in general. As train safety and risk analysis rely on
18 accurate assessment of derailment likelihood, a guide for transportation research is needed to show
19 how each technique can approximate the number of observed derailments. In this study, a new
20 stochastic mathematical prediction model has been established on the basis of a hierarchical Bayesian
21 model (HBM), which can better address unique exposure indicators in segmented large-scale regions.
22 Integration of multiple specialized packages, namely, MATLAB for image processing, R for
23 statistical analysis, and ArcGIS for displaying and manipulating geospatial data, are adopted to
24 unleash complex solutions that will practically benefit the rail industry and transportation
25 researchers.

26 **2 INTRODUCTION**

27 The majority of rail accidents are attributed to train derailments, leading to operational shutdowns,
28 financial losses, injuries, and even fatalities. A derailment takes place when a rolling stock becomes
29 unstable and leaves its rail tracks resulting from a number of causes. These include the mechanical
30 failure of turnout components, such as a worn or broken turnout frog or crossing nose. In the
31 prediction analysis of these components, GIS and Mathematical modelling of assumptions are often
32 employed. Compared to GIS, which became an option for analysing rail accidents at the beginning
33 of 2000s, mathematical modelling of accidents is quite mature in transportation engineering.

34 The earliest example on a comprehensive mathematical study of railway accident rates was
35 conducted by (Nayak, et al.) in 1983. The study deals with holistic derailment frequency and the
36 probability distribution of the number of wagons and locomotives in the US. Its estimation
37 methodology has been updated throughout several later studies with more sophisticated and specific
38 methodologies. A quantitative correlation between derailment rate and track class has been
39 discovered which considers rail traffic and the location and frequency of derailments (Treichel &
40 Barkan, 1993). Another study has enabled the probabilities of Class I and non-Class I railroad freight

41 train accidents to be determined in a more precise way for the various classes of main-line track
42 (Anderson & Barkan , 2004). Critical parameters have been revealed by utilising the US Federal
43 Railroad Administration (FRA) accident database and related literature, then analysed in order to
44 predict derailments of rolling stocks (Xiang , et al., 2011). The same research group (2017) also
45 considers the FRA track class, method of operation, and annual traffic density in order to develop
46 point estimators of and confidence intervals for derailment rates. Dindar et al. (2017) develops a
47 Bayesian mathematical model with which to identify the risks of derailments caused by extreme
48 weather conditions. The fundamental congruency between these studies on estimates of the
49 derailment rates is a comprehensive methodology which is used to estimate various kinds of failures
50 causing derailments. As train safety and risk analysis relies on accurate assessment of derailment
51 likelihood, the more precisely the number of derailments across the region is estimated, the less
52 maintenance expenses might be achieved, and the higher rail safety is provided within the region.

53 GIS has often been a preferred method for ensuring the higher rail safety , and identifying a weighted
54 combination of the cost and risk associated with derailments for a set of reasons. The cost–risk trade-
55 offs for railway shipments of hazardous materials has been studied in order to reveal some rerouting
56 problems by overlaying the rail network on a census area map using GIS techniques (Glickman, et
57 al., 2007). A quantitative risk analysis of hazardous materials, based on GIS, has been introduced to
58 evaluate tank car design, product characteristics, traffic volume, infrastructure quality, and population
59 exposure along shipment routes (Kawprasert & Barkan , 2010). Optimal frequencies for annual
60 inspections of different track segments has also been developed by using GIS to determine accurately
61 the route information for each rolling stock (Liu, 2017). Further, the impact of climate elements on
62 component failures at rail turnouts (RTs or so-called ‘switches and crossings’) has been investigated
63 by using GIS to calculate the exposure compounds (Dindar, Under review).

64 In general, mathematical models involved in the methodology of quantitative risk research might be
65 accompanied by assumptions, some more heuristic than others. The characteristics of the data, e.g.,
66 correlational trends, distributions, and variable types, are, in general, determined by these
67 assumptions. In railway risk research, many researchers have made various assumptions, particularly
68 assumptions related to a set of risk indicators, i.e., rail traffic, in order to duplicate the intended
69 research scenarios as closely as possible (Ishak, et al., 2016; Dindar, et al., 2017). The assumptions
70 have been made on the basis of statistical data which corresponds to the studies up to a point.
71 Therefore, the population, statistical tests used, research design, or other delimitations in the studies
72 are highly likely to create uncertainties in readers.

73 This study investigates to what degree such frequently made assumptions, regardless of the GIS
74 techniques used, impact the expected results. In order to do so, a region is segmented while taking
75 climate conditions into account, which is aimed at eliminating the impact of climate. In order to
76 analyse particular derailments related to component failures at railway turnouts, exposure levels of
77 each state within the segmented region are determined by means of real data and/or a set of
78 assumptions. Finally, using a comparison of the outcomes for different exposure levels, the
79 derailment rates are eventually reached through a hierarchical Bayesian model (HBM).

80 **3 DATA RELIABILITY AND USE**

81 The US Department of Transportation authorises the FRA to conduct recordkeeping and report
82 various kinds of accidents, i.e., derailments and collisions, under the regulations put forth in Title 49
83 of the Code of Federal Regulations (CFR) Part 22. The FRA uses these accident reports to identify
84 comparative trends in railroad safety and develop risk reduction and hazard elimination programs

85 associated with preventing railway injuries and accidents. One of the primary groups of accidents and
 86 incidents to be reported is rail equipment accidents/incidents. These groups will be coded throughout
 87 this study with a set of specific numbers.

88 This study investigates component failures at RTs, which are specified by the FRA codes T301 to
 89 T399. As shown in Table 1, the FRA discretises RT-related component failures into 18 types of
 90 accidents, each of which describes different failures at RTs and gives rise to various consequences.

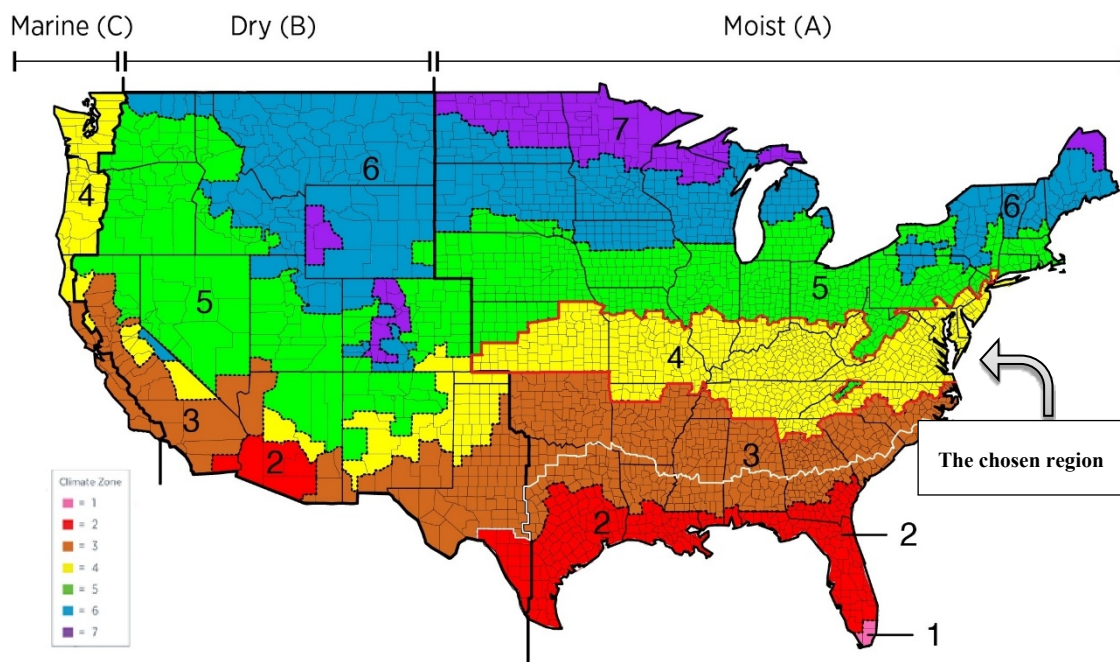
91 *Table 1 Reported Failures of Frogs, Switches, and Track Appliances at RTs*

FRA Code	Description of failure
T301	Derail, defective
T302	Expansion joint failed or malfunctioned
T303	Guard rail loose/broken or mislocated
T304	Railroad crossing frog worn or broken
T307	Spring/power switch mechanism malfunction
T308	Stock rail worn, broken, or disconnected
T309	Switch (hand-operated) stand mechanism broken, loose, or worn
T310	Switch connecting or operating rod is broken or defective
T311	Switch damaged or out of adjustment
T312	Switch lug/crank broken
T313	Switch out of adjustment because of insufficient rail anchoring
T314	Switch point worn or broken
T315	Switch rod worn, bent, broken, or disconnected
T316	Turnout frog (rigid) worn or broken
T317	Turnout frog (self-guarded) worn or broken
T318	Turnout frog (spring) worn or broken

T319	Switch point gapped (between switch point and stock rail)
T399	Other frog, switch, and track appliance defect

92

93 RTs are known to be affected considerably by environmental conditions, i.e., temperature (Dindar, et
 94 al., 2016; Sa'adin, et al., 2016). As a result, physical changes in turnout components are expected to
 95 vary from a climate region to another. Therefore, it is suggested that regional segmentation on the
 96 basis of climatic characteristics might yield better estimation (Dindar, et al., 2017; Dindar, et al.,
 97 2017; Dindar, Under review). As the study intends to investigate the impact of assumptions on the
 98 results, the elimination of the additional impact of the climate itself could be necessary. Figure 1
 99 shows the distribution of the climate zones across the US.



100

101 *Figure 1 Climate Zones in the US*

102 The US consists of seven fundamental, temperature-based zones (TBZs) and three precipitation-
 103 based zones (PBZs). The TBZs are numbered from 1 to 7, while the PBZs are divided into three
 104 groups, namely A to C. Each zone has unique variables, including precipitation, temperature, traffic
 105 density, and an intersectional variable, track class. This study will use a region composed of TBZ 4
 106 and PBZ A, which is shown in yellow, outlined in red, and positioned to the right in Figure 1. Again,
 107 the reason for choosing this particular region is to minimise the impact of climate. The following
 108 states are included in the chosen region: Arkansas (AR), the District of Columbia (DC), Delaware
 109 (DE), Georgia (GA), Illinois (IL), Indiana (IN), Kansas (KS), Kentucky (KY), Missouri (MO),
 110 Maryland (MD), North Carolina (NC), New Jersey (NJ), New York (NY), Ohio (OH), Pennsylvania
 111 (PA), Tennessee (TN), Virginia (VA), and West Virginia (WV).

112 With approximately 140,000 miles of track in total US rail service as part of the interstate railway
 113 system, the FRA and US railway operators together undertake a full monitoring of the system's

114 condition. All track is categorized into six classes, which indicate the quality of the track and are
115 segregated by maximum speed limits. This study will concentrate on derailment estimates and
116 severity on a state-by-state basis for entire networks in the chosen region. It is assumed that the
117 condition of the turnouts is distributed homogenously through the states, as the study only focuses on
118 derailments on entire tracks. However, the number of homogenously distributed turnouts in a state is
119 said to be relevant to either the length of the railway network or the density of traffic (rail ton-miles
120 per track mile per year¹). Although the former would yield unrealistic results by considering the
121 possibility of different counts of turnouts due to a large network, this paper leans towards the use of
122 both the former and letter, which better offer reasonable information on to what degree turnouts on
123 the entire network have exposure to any kind of rolling stock even under assumptions. Aside from
124 the rail traffic measure in this region, the number of turnouts is assumed to be homogenously
125 distributed. It is deterministically identified that there is one turnout² per 1.18 track mile (see Section
126 4.4.2) [17].

127 Regarding real data of density of traffic, a conventional method for measuring the rail traffic over a
128 rail section, used mostly by the rail industry, is MGT, which is found by using ArcGIS. As this paper
129 only focuses on turnouts (or ‘switches and crossings’), the traffic over a turnout (instead of a section
130 of rail) is used to calculate MGT-based rail traffic. Therefore, the measure of the MGT of traffic is
131 based on the cumulative total static weight (including rail cars and locomotive or locomotives) of the
132 traffic passing over a turnout within a year. MGT will be used as a unit of real data and as an
133 assumption, which leads to a direct comparison between real data and mathematically-generated data.
134 On the other hand, the measure of carloads, which is only used for an assumption, is obtained by
135 counting the number of car which pass through carrying goods. In addition to carloads, rail ton-mile
136 is also used to assume exposure to segmented regions, posing as the entire chosen region . This is
137 another unit of rail traffic and is the equivalent of shipping one ton of product per one mile without
138 considering any other kind of static weight, such as those of the locomotive and car. Both rail ton-
139 mile and carloads will be compared to MGT in order to see how the estimation of derailment counts
140 is achieved approximately through them.

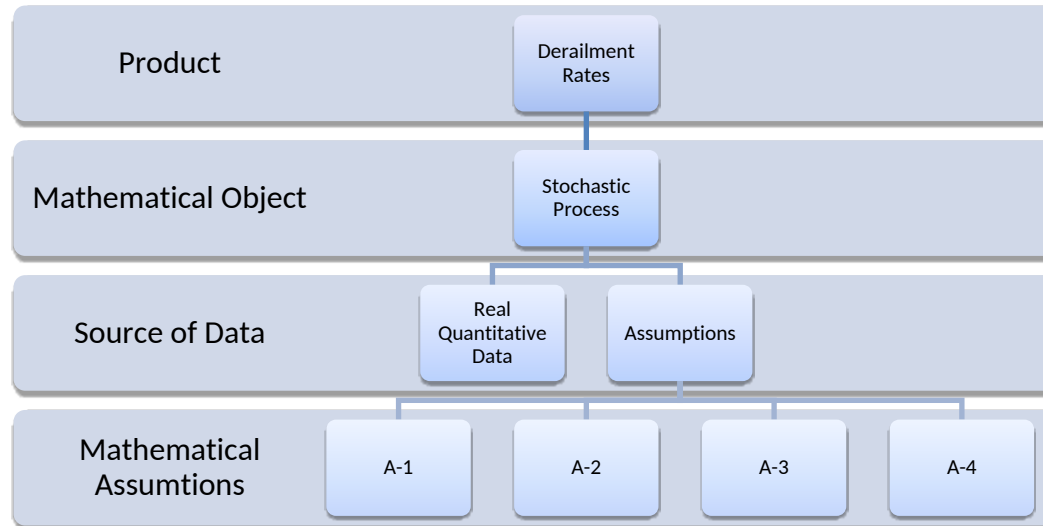
141 4 METHEDODOLOGY

142 4.1 Structure

143 The outline of the work is illustrated in Figure 2, which is composed of three technical phases. The
144 overall aim is firstly to obtain derailment rates, by using different data sources, through different
145 mathematical modelling techniques. Secondly, a comparable statistical analysis is achieved to
146 benchmark the obtained derailment rates.

¹ This is the product of the annual total weight (including the weight of locomotives and loaded/unloaded wagons) and the distance moved by a rolling stock.

² The number of turnouts is determined only considering the number of switches in a rail section. For instance, a single crossover, consisting two switches, is described as two turnouts positioned in two tracks.



147

148 *Figure 2 Phases of the Research*

149 In order to fulfil a critical role in the achievement of the research objectives, stochastic process as a
 150 mathematical object is used. This is a novel mathematical process used to identify the distribution of
 151 the derailment rates at a given time with random variables, in contrast to a deterministic process built
 152 on derailment counts, rail traffic, and the number of rail turnouts. Data sources, i.e., real quantitative
 153 data (RQD) and assumptions, are outlined throughout the subsections below. The first three
 154 mathematical assumptions (A-1, A-2, and A-3) are associated with different units of rail traffic
 155 (million gross tonnes (MGT), rail ton-mile, and carloads, respectively), and the other assumption (A-
 156 4) refers to the number of turnouts, which is another risk indicator.

157

158 4.2 Engineering Assumptions

159 4.2.1 Exposure Indicators

160 In order to exclude environmental factors, the segmentation of the states is executed in accordance
 161 with climate patterns. As the density of the rail traffic and the number of rail turnouts within all of
 162 the segmented states are considered when investigating the number of derailments, both are
 163 considered to be exposure indicators in this study. To be more precise, the traffic density of a railway
 164 network influences considerably train safety and risk analysis and thereby leads to fluctuations in
 165 derailment rates. On the other hand, the more turnouts a rail network within the region possesses, the
 166 higher the expected number of derailments at turnouts.

167 It should be noted that the number of derailments is associated with some metric of traffic exposure
 168 indicators, such as car-miles, train-miles, gross ton-miles, or rail tonnes (Dindar, et al., 2016). As
 169 described in Section 3, MGT, carloads, and train-miles are presumed to be associated with the
 170 derailment of freight trains in this study.

171 *Table 2 Normalised Exposure of RTs to Derailments in the Selected Region*

	Illinois	Kansas	Nebraska	North Dakota	Oregon	Texas
TND	57	25	16	2	2	78
AATV	503.1	344.6	511.1	128.1	54.4	373.4
TRMS	6,986	4,855	3,375	3,330	2,396	10,469
NED	3,514,657	1,673,033	1,724,963	426,573	130,342	3,909,125

172

173 Table 2 shows various statistical patterns and risk indicators, e.g., the normalised exposure to
 174 derailment (NED). To obtain such a normalised exposure, the average annual traffic volumes
 175 (millions of tons) (AATV) of states might be presented as the first indicator of derailments. On the
 176 other hand, the number of RTs in a particular state is assumed, on average, in accordance with the
 177 values of TRMS (Total Rail Miles by State). That is, the number of turnouts might be correlated with
 178 the length of the rail network which a state possesses. The NED has been investigated through the
 179 product of these two indicators, AATV and TRMS. The total number of derailments (TND) is also
 180 seen to be a logical response to the output of this product.

181 It is worth noting that other sets of circumstances, e.g., weather conditions, speed, vehicle type,
 182 maintenance level, and time frame, have some effects on turnout-related derailments. However, the
 183 chosen region provides a useful, simplified way of reducing the effects of those indicators. Firstly,
 184 the region has the same weather characteristics throughout, and, secondly, might be considered to be
 185 quite large enough to exhibit a homogenous distribution of vehicle type over the given five-year
 186 period. It is important to keep in mind that derailments caused by speeding have been placed in
 187 another group of causes in FRA reports and that this study only focuses on turnout component
 188 failures that account for major causes of the turnouts-related derailments.

189 4.2.2 Assumptions on Indicators

190 The applied traffic pattern in the model, which will be identified later, might be expressed either in
 191 terms of a conventional method for measuring the traffic over a section of track used in the rail
 192 operation (MGT) or in terms of the number of wagons passing by, carloads. To be precise, the latter
 193 is the cumulative total of the static load over a section of engaged track, while the former is
 194 associated with the quantity of rolling stocks passing through a given section of rail track without
 195 considering how much weight is transported.

196 As indicators for a unit of rail traffic and the number of turnouts are investigated in order to
 197 comprehend their impacts on derailment rates, the following assumptions are necessary:

- 198 • A-1: as will be shown in Section 4.2.3., MGT traffic values contributed by each state to the
 199 given region (see Fig. 1) are calculated based on this assumption that the distribution of the
 200 MGT traffic values is homogeneous throughout the states.
- 201 • A-2: the rail ton-miles contributed by each state to the given region (see Fig. 1) are calculated
 202 assuming that the distribution of rail-ton miles is homogeneous throughout the states.

203 • A-3: the process established by A-1 & 2 is followed; however, the carload values are analysed
 204 as a traffic indicator instead and their distribution is assumed to be homogeneous throughout
 205 the states.

206 On the other hand, the number of turnouts, another exposure indicator, uses:

207 • A-4: a flowchart, suggested in Figure 2, is applied to distribute the number of turnouts across
 208 the chosen region. The length of rail network is assumed to be associated with the number of
 209 turnouts.

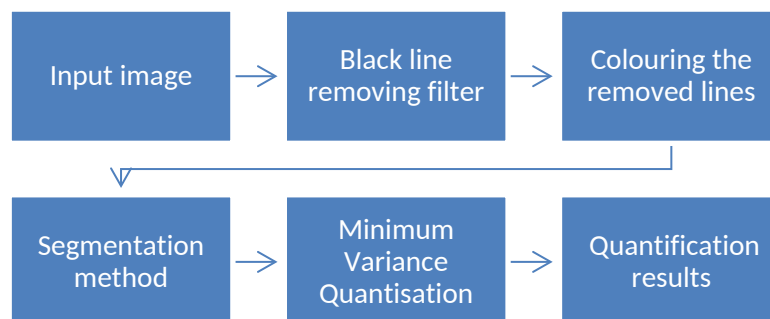
210 The data for the calculations for A1- A3 is obtained from the Association of American Railroads
 211 (AAC, n.d.). This source is only used for these three assumptions. At first glance, such assumptions
 212 might not be expected to help yield derailment rates. However, one of the aims of this study is the
 213 identification of which indicator yields better rates under given circumstances.

214 4.2.3 Area Calculation for the Regions

215 Seven US climate regions have been introduced and outlined in Section 3. In accordance with the
 216 different climate regions in Figure 1, different coloured layers are used for forecasting the expected
 217 relation between natural phenomena and railway component failures. In order to reveal this, a new
 218 mathematical model will be essential to the stochastic model establishment (see Eq-2 and Eq-3).

219 This subsection will investigate what proportions of the states identified in Section 4.2.1 fall into the
 220 chosen region. Image processing is firstly conducted through MATLAB. Although image processing
 221 has become popular in railway engineering, the applications have been limited to remote sensing
 222 (Dindar, et al., 2017). Thus, this paper, might be said to be following a different approach by using it
 223 to consider regional exposure to the risk of derailment.

224 The framework for the segmentation and quantification of the states is illustrated in Figure 3. The
 225 first phase in this framework is the input image, which projects the climate regions on the states, as
 226 shown in Figure 1. The input image includes black lines used to distinguish all of the regions, states
 227 and some counties from each other. Those black lines are then removed and filled in equally with the
 228 two neighbour colours. Then, a set of masking techniques are performed through the MATLAB
 229 toolbox, as illustrated in Figure 4.



230

231 *Figure 3 Flowchart of the Framework for the Quantification of the Climate Zones*

232

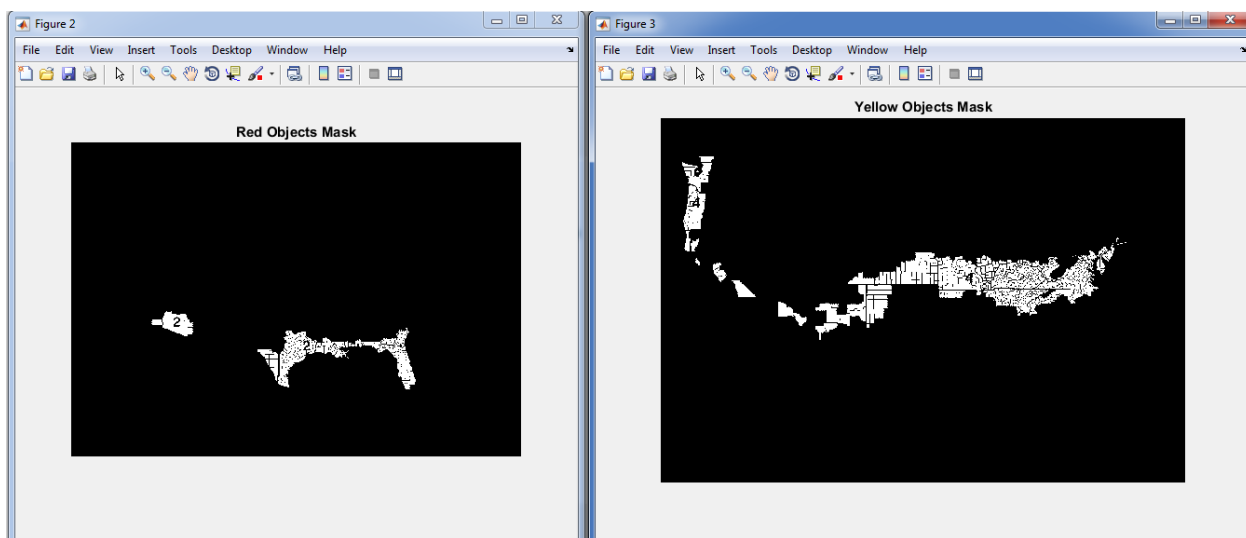
233 In the fifth step, known as Rgb2ind^3 , the maximum number of colours is specified in the output
 234 image's colormap to perform a minimum variance quantization. The numbers are selected to
 235 determine the number of boxes into which the RGB colour cube (R, G, B) indexed image (consisting
 236 of 255 colours) is separated. As result, the areas of all climate zones along with the test states are
 237 reached, and the findings are presented in Table 3.

238 *Table 3 Quantification Results for the Climate Zones*

Climate zones	Colour	Decimal Code (R, G, B) ^{4, 5}	Pixel Count	Proportion of sizes
1	Pink	(255, 105, 182)	500	0.001
2	Red	(255, 0, 0)	27,575	0.051
3	Brown	(210, 105, 33)	116,157	0.214
4	Yellow	(255,255,0)	48,369	0.089
5	Green	(0,245,0)	169,511	0.312
6	Blue	(0,155,205)	144,744	0.266
7	Purple	(0, 155, 240)	37505	0.069

239

240 Using an Intel ® Core™ i7 -6700 HQ processor, it took approximately 35 minutes to execute
 241 2,000,000 pixels within the image through MATLAB.



242

243 *Figure 4 Area Segmentation Samples for Climate Regions*

244

³ a MATLAB function which converts the RGB image into an indexed image X using minimum variance quantization and dithering.

⁴ The RGB values in the column are extracted from the image, which means that any value might only be addressed with the corresponding colour in the proposed map.

⁵ The RGB values are coded within an interval of plus-and-minus 5.

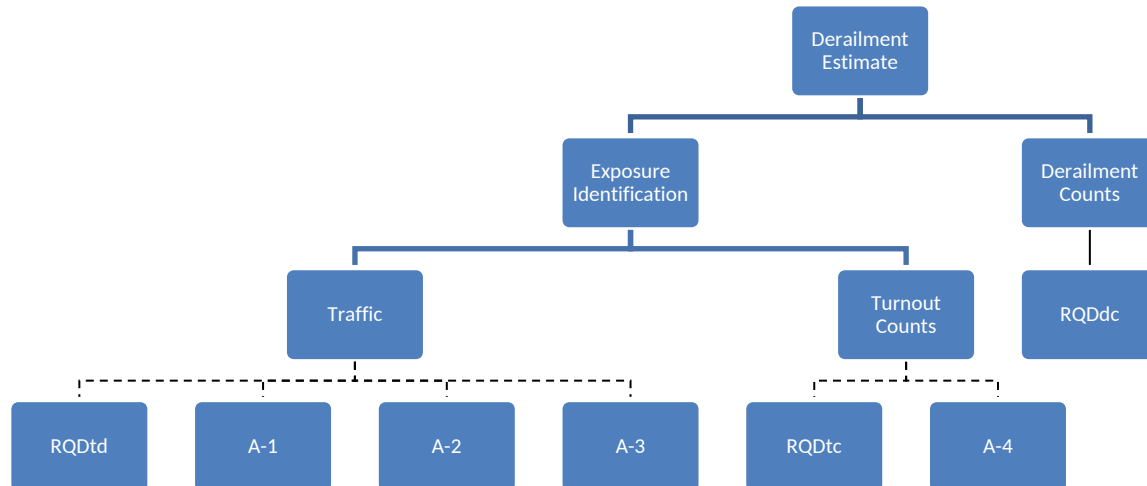
245 4.3 Identification of Risk Exposure Indication Combinations

246 In order to better understand the effect of the new mathematical modelling on the risk exposure by rail
 247 transport to derailment, this study is designed to assess the performance of various assumptions against
 248 real data. Therefore, combinations of assumptions (traffic units and turnout counts) are required in
 249 order to perform the investigation. Figure 5 illustrates the entire structure to which the research has
 250 been applied. Dotted lines in the structure are used to express that only one box in the branch is utilised
 251 as an information source, whereas straight lines stress that mathematical equations, using all the data
 252 in the branch, are required to continue upward.

253 To clarify the figure in detail, the traffic indicator is selected among four data sources, namely, A-1 to
 254 3, and RQD_{td} ⁶, while either A-4 or RQD_{tc} ⁷ is used as an additional data source. Throughout Eq-2 (see
 255 Section 4.4), the exposures of segmented regions are calculated with the chosen data source. Derailment
 256 estimates, then, are calculated using the exposures and real derailment counts by means of
 257 Eq-5 (see Section 4.4.). Therefore, as the selections of two different kinds of indicators within the two
 258 sets in which order is regraded are matched, eight combinations of two indicators can be drawn from
 259 these two indicator sets: RQD_{td} and RQD_{tc} (R_1), RQD_{td} and A-4 (X_1), A-1 and RQD_{tc} (X_2), A-1 and
 260 A-4 (X_3), A-2 and RQD_{tc} (X_4), A-2 and A-4 (X_5), A-3 and RQD_{tc} (X_6), and A-3 and A-4 (X_7).

261

262



263

264 *Figure 5 Structure for the use of the Assumptions and Real Database*

265

⁶ Real quantitative data for rail traffic density.

⁷ Real quantitative data for turnout count.

266 4.4 Comparable Model Development

267 To conduct an analysis on the component failure rates at RTs and understand the precision of the
 268 mathematical assumptions on risk exposures, it is necessary to appoint a novel stochastic model,
 269 which is capable of estimating the rates of the derailment accidents within the chosen zone as
 270 effectively as possible. The novel model is required to respond both to real exposure values (the
 271 number of turnouts and traffic volume) and the values created by a set of assumptions using inexact
 272 data.

273 The structure of the model, therefore, is composed of a fixed formula, which is capable of addressing
 274 various kinds of exposure. Hierarchical modelling has been suggested to precisely estimate
 275 derailment rates of component failures at RTs in a given region (Dindar, et al., 2019). The
 276 modification of the suggested model (Albert, 1988) is illustrated in Eq.1.

277

$$p(\alpha, \mu | data) = \kappa \frac{z}{\Gamma^6(\alpha) (\alpha + z)^2 \mu} \sum_{i=1}^{18} \left(\frac{(\alpha^\alpha \mu^{-\alpha}) \Gamma(\alpha + \lambda)}{(\alpha/\mu + \pi)^{(\alpha + \lambda)}} \right) \quad (1)$$

278

279 where α and μ are hyperparameters of a gamma function, κ is a proportionality constant, and i
 280 indicates state i within the chosen region. The verification of the model had been achieved (Albert,
 281 1999). Thus, it can be identified that the marginal posterior density of (α, μ) is discovered through
 282 the suggested equation. Also, as the chosen region is made up of proportions from 18 different states,
 283 $i = 1, \dots, 18$. That is, each state contributes unequally to the marginal probabilities. Further, an
 284 MCMC algorithm is used to find a kernel density estimate of the simulated draws from the marginal
 285 posterior distribution (Albert, 1996).

286 In addition, π in Eq.1 is found by

$$\pi_i = e_i \cdot \lambda_i, \quad (2)$$

287 where λ denotes the occurrence rate in a given state (A-1, A-2 or A-3), and e (A-4) is the exposure
 288 (per year). The mathematical formula for the exposure is shown below.

289

$$e_i = \sum_i^{18} w_i \cdot TRMS_i \cdot AATV_i, \quad i = 1, \dots, 18, \quad \forall i \in \mathbb{N}, \quad (3)$$

290 where w_i is the proportion of the area corresponding to i th state in the assigned climate, $i = 1, \dots, 18$.
 291 For instance, if a quarter of the area that a state possesses falls into the chosen region, then w_i is 0.25.

292

$$\lambda_i = \sum_i^{18} w_i \cdot \lambda_i, \quad i = 1, \dots, 18, \quad \forall i \in \mathbb{N}, \quad (4)$$

293 where λ_i represents occurrence rate for the proportion of i th state situated on the region. The
 294 acquisition of the occurrence rate (λ) corresponding to the chosen region follows a process equivalent
 295 to that used for the acquisition of the exposure (e). That is, after determining a constant value of w_i
 296 for i th state, the values of e and λ associated with this state are found by using Eq-3 and Eq-4. In
 297 addition, Eq-3 and Eq-4 are used for the assumptions (see Section 4.1). Eq-1 through Eq-5 consist of
 298 the second level of the hierarchical model. The first level is then simplified in the following equation
 299 in order to obtain derailment rates which are sampling from a gamma ($\alpha, \alpha/\mu$) distribution of the
 300 form.

301

$$g_1(\lambda | \alpha_1, \mu) = \frac{1}{\alpha_1 \Gamma(\alpha_1)} \left(\frac{\alpha_1}{\mu} \right)^{\alpha_1} \exp(-\alpha_1 \lambda / \mu), \quad \lambda \in [0, +\infty), \quad (5)$$

302 where α_1 is the prior parameter of an inverse gamma function with hyperparameter α (Albert,
 303 1999). On the other hand, the state with the smallest estimated derailment rate for each combination
 304 can be identified through the following formula:

305

$$E \left(\frac{\text{derailment count} + \alpha_1}{\pi + \left(\frac{\alpha_1}{\mu} \right)} \right) \quad (6)$$

306

307 5 RESULTS

308 To both understand the performance of the assumptions compared to the real database and analyse
 309 the impacts of the assumptions on estimation of turnout component failures, the proportion of each

310 state within the region is firstly computed. Table 4 has been established by the methodology
 311 presented in Section 4.2.3. It exhibits the complete details of the observed data and prediction. The
 312 mathematical modelling has then been expanded to include the other two units of rail traffic, namely,
 313 rail ton-miles and carloads. As observed, some prediction models underperform compared to the
 314 RQD. Some relatively small proportions of states in the region, such as the proportions from AR and
 315 NY, have assumptions which diverge from RQD, while the remaining states' assumptions, e.g. DC,
 316 DE, and NJ, do well for the most part. Regardless of either how large or small the proportions from
 317 the states are or how much rail traffic is present in the states, an assumption which is based on
 318 turnout counts seem to fluctuate widely.

319

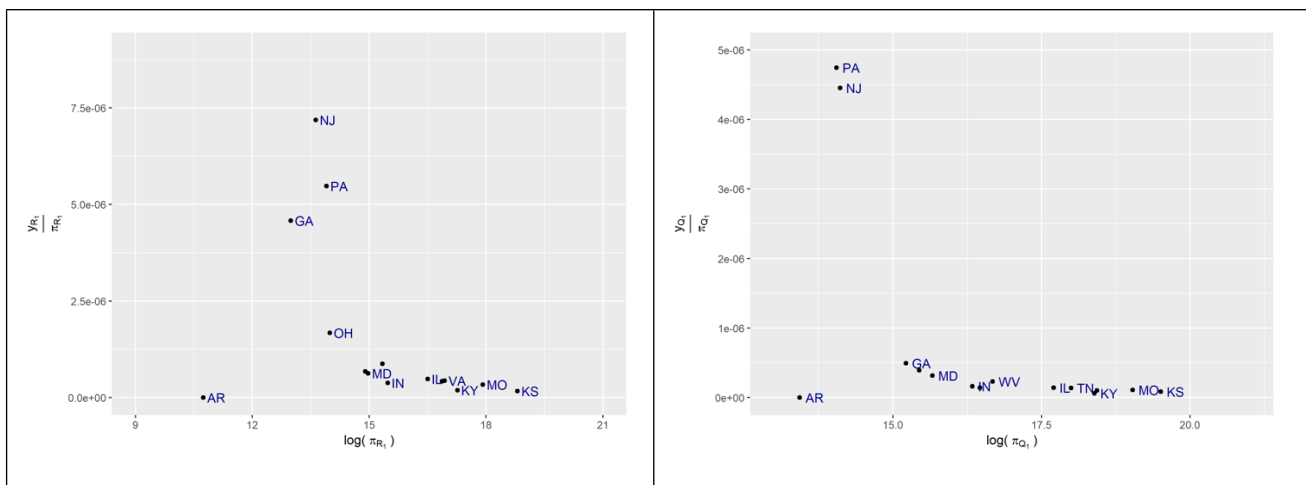
320 **Table 4 Derailment-Risk Indicators for the States Located in the Chosen Region.**

	Rail Traffic				Turnout Counts	
	ArcGIS	Predictions			ArcGIS	Predictions
States	RQD _{td} (MGT)	A-1 (MGT)	A-2 (Rail ton- miles)	A-3 (Carload)	RQD _{tc}	A-4
Arkansas	701	4341	34	549527	66	969
The District of Columbia	320	320	32	584800	319	36
Delaware	438	478	17	310600	145	450
Georgia	3730	2099	24	531664	117	1090
Illinois	11549	18643	170	4035137	1272	4237
Indiana	5356	8809	91	2156692	989	2321
Kansas	50510	35102	231	4120533	2914	5862
Kentucky	20668	20678	252	4351700	1526	4694
Maryland	5144	4743	81	1879260	620	1234
Missouri	35543	33979	311	5944221	1703	5201
North Carolina	5037	5713	40	695750	590	2812
New Jersey	1294	1163	26	883979	645	1041
New York	40	339	1	35286	190	130
Ohio	4151	6333	37	848620	288	1228
Pennsylvania	1747	2016	15	340029	627	724
Tennessee	17143	15856	179	3242668	1243	3822
Virginia	17489	17486	159	2851607	1301	5786
West Virginia	9907	5899	85	1385896	464	1764
Total	190766	183996	1786	34747969	14697	43401

321

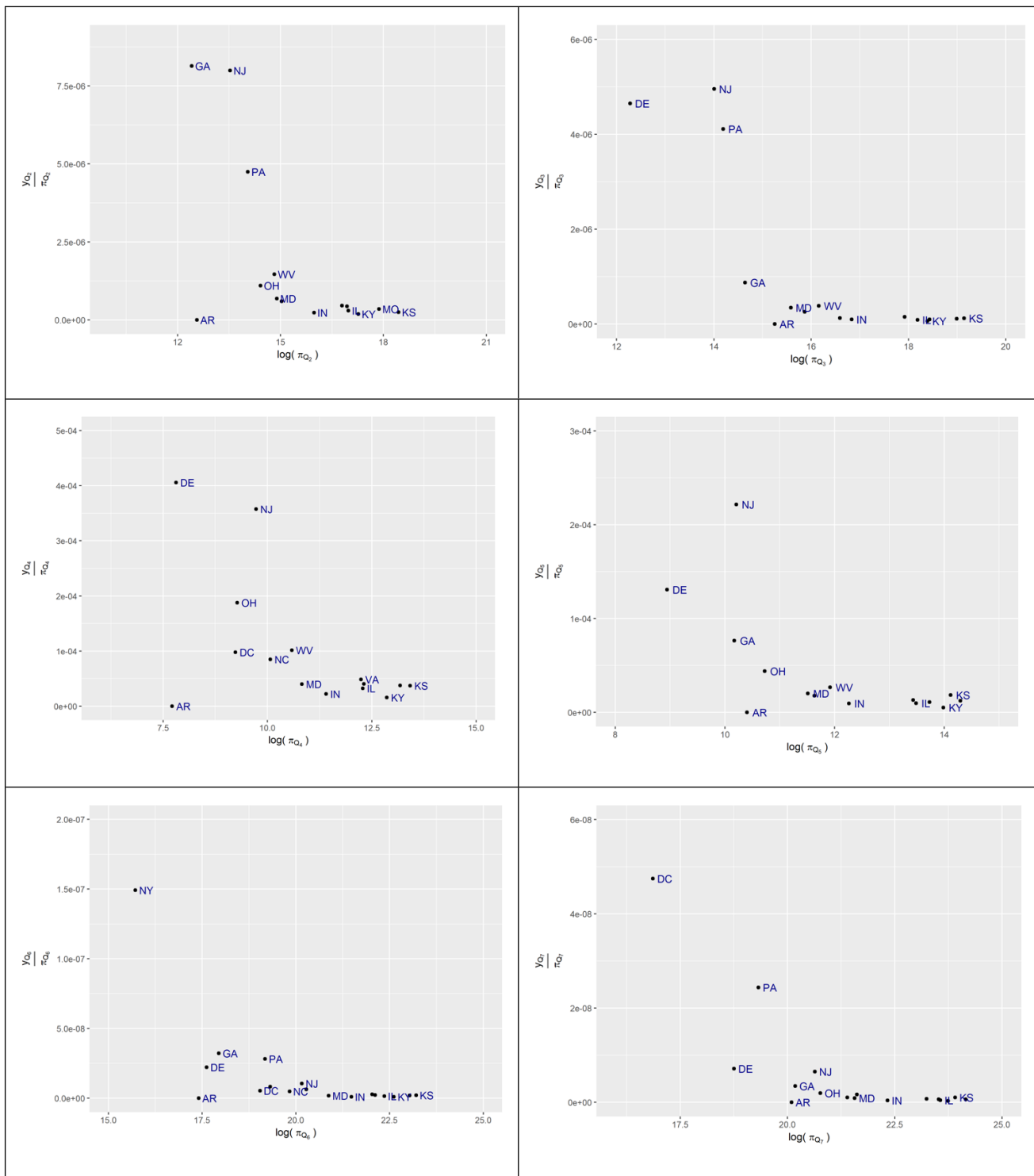
322 Based on the results shown in Table 1, any quick decision for estimation of the derailments might not
 323 be advisable. The maximum likelihood method (MLE), a method which determines values for the
 324 parameters of a model, is used to reveal the impact of the states on derailment counts on logarithmic
 325 x-axis in Figure 6. That is, the objective herein is to estimate the turnout-related derailment rates per
 326 unit of unique exposure (λ) which each state has. Thus, the MLEs $\left(\frac{y}{\pi}\right)^{\beta}$ for the chosen states show
 327 obvious inconsistencies through each combination of exposure indicators. In general, New Jersey,
 328 Pennsylvania, and Georgia can be considered to not be at high risk of derailments considering their
 329 low turnout counts and rail traffic. It is worth noting that changes in the log exposure (x-axis) cannot
 330 be compared as the unit of exposure indicators vary throughout the combinations. However, this
 331 kind of estimate is open for discussion, as derailment events at turnouts, in particular those caused by
 332 component failure, are rare⁹. To remedy such a situation as much as possible, a Bayesian estimate,
 333 based on prior knowledge of the derailment rates, is used as shown in Section 4.4. As shown in
 334 Figure 6, the fact that a number of MLEs are placed at a low scale might also be expressed as proof
 335 of the necessity of performing a hierarchical Bayesian analysis.

336



⁸ The number of derailments per unit exposure

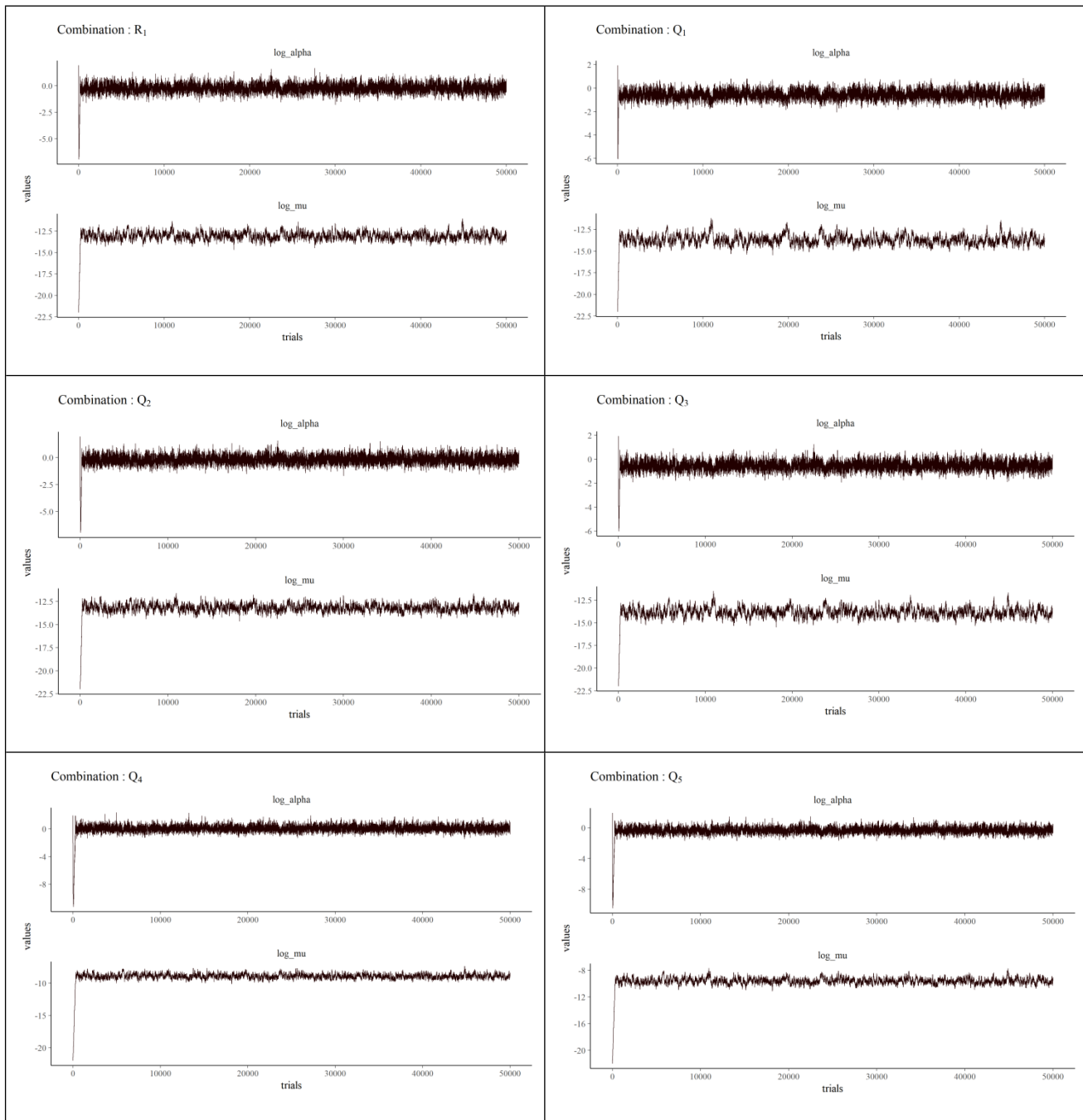
⁹ Due to nature of MLE, as the number of derailments (y_i) becomes smaller, the estimate becomes worse. Moreover, if any derailment does not occur in a chosen region, it might still be quite unwise to bet that the estimate in question will never occur in the future.



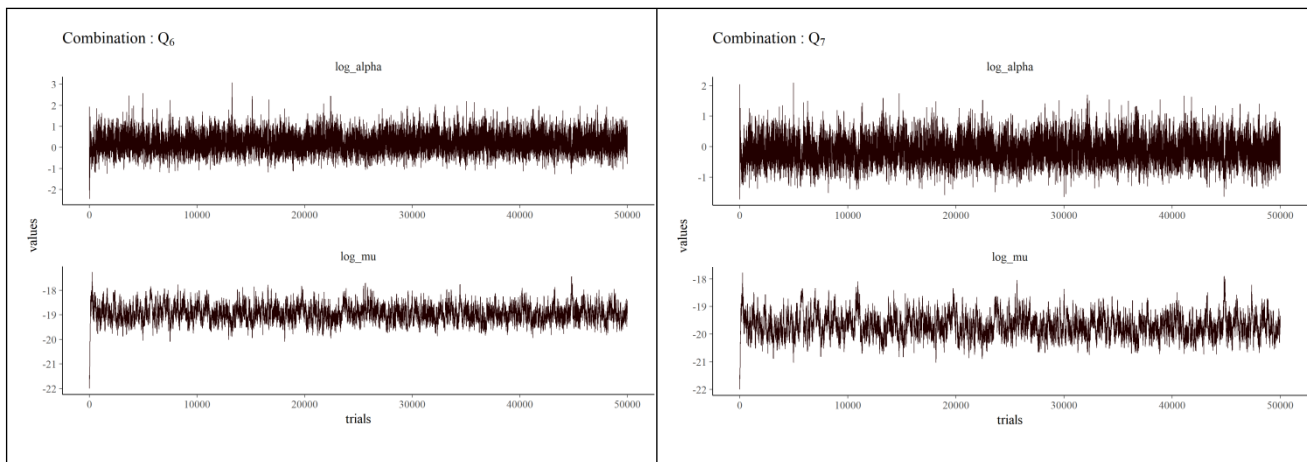
337 **Figure 6 MLE Estimates for the Chosen States**

338 Hyperparameters (α and μ), which are nested on the first floor of the structure (see Eq.5), must be
 339 simulated using the marginal posterior distribution. It is noted that the posterior density for ($\log \alpha$,
 340 $\log \mu$) is not shaped in a desired way. The normal approximation to the posterior, therefore, is

341 insufficient for proper simulation. Metropolis within the Gibbs algorithm¹⁰ allows the log-
342 hyperparameters to be simulated. The initial trials in the simulation for the two conditional
343 distributions for each combination have been assigned the equivalent starting point (-5, -22). The
344 acceptance rates in the simulation are limited to 20%, and the number of iteration in the simulation is
345 50,000. Figure 7 illustrates the simulation trace plots for the assigned values of the hyperparameters
346 (α and μ) from the Bayesian hierarchical model.

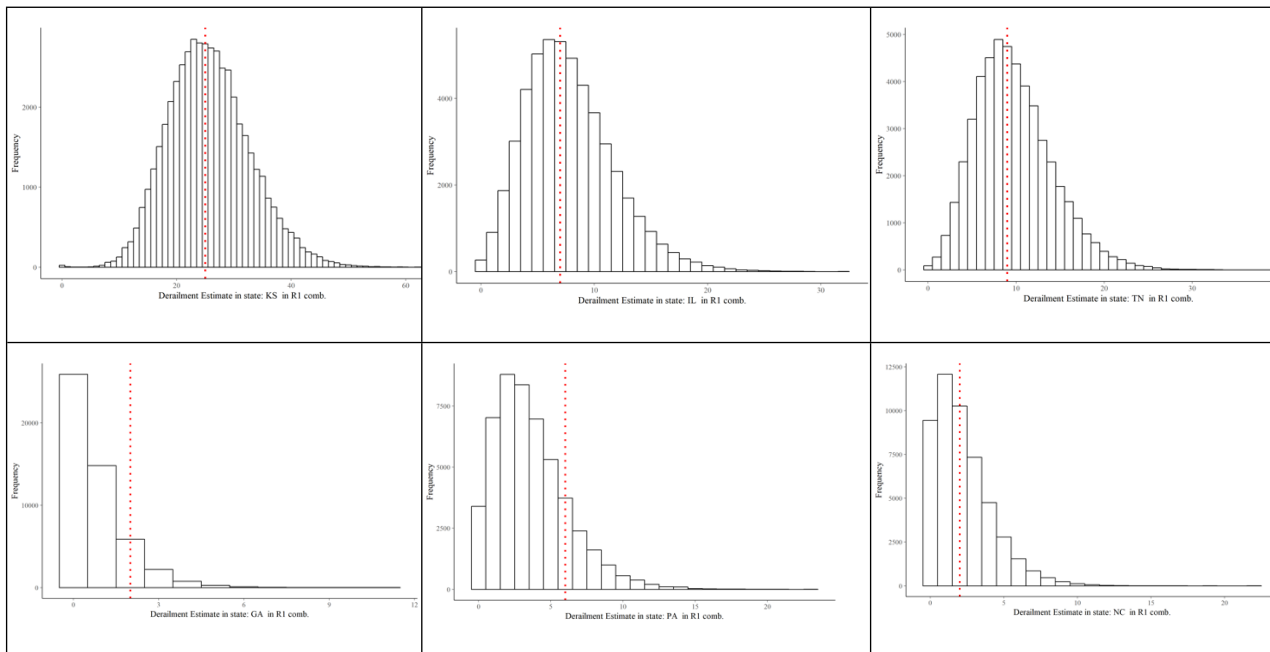


¹⁰ Available at <https://www.rdocumentation.org/packages/LearnBayes/versions/2.15.1/topics/gibbs>



347 **Figure 7 Trace Plots of the MCMC Sampling Procedure for the combinations of $\log(\alpha)$ and $\log(\mu)$**

348 As seen in the traces for the combinations Q6 and Q7 (fully formed by assumptions) in Figure 7, there
 349 are wide fluctuations present, likely as derailment exposure indicators show inconsistency through the
 350 states.



351 **Figure 8 The number of Observed Derailments (red dotted line) and Histograms of the Simulated**
 352 **Draws from the Posterior Predictive Distribution for Several States for R1**

353 The more symmetric the simulated draws on the right and left tails of the number of observed
 354 derailments are, the better the estimate. For instance, the first three histograms in Figure 8 indicate the
 355 robustness of the hierarchical model, while the distribution for GA does not. However, the estimate is
 356 seen to deviate slightly in regions with low numbers of derailments, which does not affect substantially
 357 the number of derailments in population, as the entire region has 107 derailment cases.

358 **Table 5 Descriptive Statistics for the Bayesian Hierarchical Model Assigned with Various**
 359 **Exposures for the New York Rail Network¹¹**

	Min	Q_1	μ_{NY}	Q_3	Max	σ_{NY}	W^-	W^+	\hat{p}_1	$\hat{p}_{0,1,2}$
R1 _{NY}	0	0	0.03432	0	3	0.1902179	0.02994607	0.03300592	0.03144	0.99998
X1 _{NY}	0	0	0.02144	0	4	0.151726	0.01859588	0.0210379	0.01978	0.99994
X2 _{NY}	0	0	0.238	0	6	0.5387683	0.1560788	0.1624935	0.15926	0.9931
X3 _{NY}	0	0	0.1455	0	5	0.4181237	0.1039449	0.1093555	0.10662	0.99726
X4 _{NY}	0	0	0.0512	0	3	0.2308671	0.0450225	0.04872713	0.04684	0.99988
X5 _{NY}	0	0	0.02758	0	5	0.1710553	0.02421271	0.02698019	0.02556	0.99994
X6 _{NY}	0	0	0.07128	0	3	0.2727648	0.06186831	0.06615868	0.06398	0.99997
X7 _{NY}	0	0	0.03484	0	3	0.1908583	0.03070778	0.03380409	0.03222	0.99994

360

361 Table 5, for instance, shows some statistical outcomes of simulated draws for New York Rail Network,
 362 which has a low number of derailments ($Y_{NY} = 1$). Probing μ_{NY} (mean of the draws) and σ_{NY} (standard
 363 deviation of the draws), all of the combinations are said to be clustered around 0, which is not desired,
 364 as one derailment is reported in the region. Therefore, the actual coverage probability close to the
 365 nominal value of (W^-, W^+) is satisfying. However, as this particular derailment case is rarely
 366 observed, the point estimate for the actual count of the reported derailments, \hat{p}_1 , is extended with the
 367 probability of zero derailments or two derailments $\hat{p}_{0,1,2}$. As expected, R1_{NY} yields the best outcome
 368 with a probability of 0.99998. The other combinations, however, are not poor estimates.

369

11 Min and Max: the minimum and maximum intensity values at the histogram, respectively.

Q1 and Q3: the values that cut off the first 25% and 75%, respectively, of the data when it is sorted in ascending order.

σ_i : standard deviation of derailment probability values for given i th state.

W^- and W^+ : a confidence interval for a proportion in a statistical population of derailment probability values

\hat{p}_i : the proportion of the point estimate for the actual count of the reported derailments to the whole

$\hat{p}_{i-1, i, i+1}$: the proportion of the point estimate for the actual observation along with the two nearest estimations to the whole

370 **Table 6 Descriptive Statistics for the Bayesian Hierarchical Model Assigned with Various**
 371 **Exposures for the Illinois Rail Network**

	Min	Q_1	μ_{IL}	Q_3	Max	σ_{IL}	W^-	W^+	\hat{p}_1	$\hat{p}_{6,7,8}$
R1 _{IL}	0	5	7.592	10	32	3.919311	0.1012163	0.1065646	0.10386	0.30908
X1 _{IL}	0	5	7.511	10	30	3.86311	0.1021653	0.1075354	0.10482	0.32068
X2 _{IL}	0	5	7.705	10	34	3.907449	0.1046964	0.1101239	0.10738	0.32260
X3 _{IL}	0	5	7.517	10	33	3.852057	0.1043998	0.1098206	0.10708	0.32424
X4 _{IL}	0	5	7.792	10	32	3.919311	0.1035692	0.1089713	0.10624	0.31970
X5 _{IL}	0	5	7.604	10	39	3.894708	0.1027783	0.1081624	0.10544	0.32190
X6 _{IL}	0	5	7.972	10	32	3.940043	0.1017303	0.1070905	0.10438	0.31486
X7 _{IL}	0	5	7.741	10	35	3.920828	0.1043800	0.1098004	0.10706	0.32066

372

373 Considering the regions, which are expected to have higher derailment rates, Tables 6 and 7 illustrate
 374 the statistical outcomes of the given combinations. X7, which is made up of two assumptions (A-3 and
 375 A-4) and X6, which is made up of real data and an assumption (RQD and A-4), yields the worst
 376 estimates. Derailment rates in Kansas, which has one of the largest rail networks and the heaviest rail
 377 traffic in the chosen region, show that the \hat{p}_1 and $\hat{p}_{24,25,26}$ values, in particular for X6 and X7, deviate
 378 by 25 percent in comparison with R1.

379

380 **Table 7 Descriptive Statistics for the Bayesian Hierarchical Model Assigned with Various**
 381 **Exposures to the Kansas Rail Network**

	Min	Q_1	μ_{KS}	Q_3	Max	σ_{KS}	W^-	W^+	\hat{p}_1	$\hat{p}_{24,25,26}$
R1 _{KS}	0	21	25.84	30	74	7.176168	0.05486403	0.05892406	0.05686	0.16744
X1 _{KS}	0	21	25.55	30	62	7.121259	0.05164026	0.05558833	0.05358	0.16118
X2 _{KS}	0	21	25.73	30	70	7.164428	0.05486403	0.05892406	0.05686	0.16672
X3 _{KS}	0	21	25.48	30	62	7.130782	0.05631929	0.06042857	0.05834	0.16706

X4 _{KS}	0	21	25.71	30	63	7.146079	0.05382199	0.05784626	0.05580	0.16664
X5 _{KS}	0	21	25.49	30	67	7.146889	0.05311430	0.05711406	0.05508	0.16970
X6 _{KS}	0	21	25.8	30	62	7.163830	0.04832036	0.05214875	0.05020	0.14914
X7 _{KS}	0	21	25.5	30	63	7.089469	0.04512061	0.0488290	0.04694	0.13756

382

383 **6 DISCUSSION**

384 A risk quantification based on a Bayesian hierarchical model is a novel technique for conducting safety
385 analysis in railway engineering and gives rise to a huge potential in terms of railway applications across
386 many engineering domains. This paper argues that there are differences in the various mathematical
387 assumptions used as risk indicators and uses both these and recorded observations in a derailment risk
388 analysis which concentrates on component failures at RTs. The outcomes enable to be more precise
389 derailment estimation, allowing for a concrete risk rail management. As a result, the potential for severe
390 consequences is able to be minimized through better understanding the factors influencing train
391 derailment associated with this kind of failures. This study; therefore, meets the need for the judgment
392 of effectiveness and feasibility of assumptions, as one of the influencing factors. The proposed
393 methodology uses a real dataset (obtained with ArcGIS) and three different assumptions (consisting of
394 mathematical methods) for measuring the density of traffic over turnouts and one real dataset (obtained
395 with ArcGIS) and one assumption (consisting of a mathematical method) for the number of
396 derailments. To eliminate climate impact on derailment counts, a large enough region is determined by
397 considering official climate reports. Eighteen states, each with a different level of risk exposure, are
398 included in the region to be investigated. Their risk indicators, hence, risk exposures, are calculated
399 throughout either using a real FRA database or mathematically-generated databases (assumptions) or
400 a combination thereof. Then, the least to most risky three states are selected to consider the outcomes.
401 Based on a well-established Bayesian hierarchical model, comparisons of the advantages and
402 disadvantages between the use of real data and assumptions or combinations thereof are as follows:

- 403
- 404 • From the perspective of the regions with quite low risk indicators, e.g. NY, the assumptions
405 yield derailment estimate rates around the actual observations in this region. However, all of
406 the estimates seem to be incapable of calculating an estimate for a low number of derailments
407 and are identified as the most sensitive estimates in such regions. The primary reason for this
408 unreliable estimate by each combination is a scarce data environment within the risk indicators
409 and low derailment counts. To overcome this, it might be suggested that the time period selected
410 for derailment analysis be extended. Derailments, which occurred over the last five years, were
411 taken into account in this study. As the number of derailments increases, the more precise
412 outcomes should become. In other words, sampling should represent a subset of all data. To
413 satisfy the sampling analysis, 50,000 derailment samples were generated, which seems to be
414 enough to reach a conclusion, by considering the smooth distributions of bars in Figure 8. Onn
415 the other hand, as such small regions do not impact concretely the estimate of the total number
416 of derailments in the entire region, the cumulative number of derailments might be obtained in
417 the desired fashion.

- 418 • From the perspective of the regions with moderate-risk indicators e.g. Illinois¹², it is determined
 419 that it is possible for a precise estimate of the derailment rates to be determined under any
 420 uncertainty, which might be formed by the assumptions. It is worth noting that this study is
 421 conducted on the basis of a hierarchical Bayesian model estimating the parameters of the
 422 posterior distribution of turnout-related derailments in two stages. By using this advanced
 423 technique, additional evidence on the prior distribution can be acquired. The technique allows
 424 for a novel prediction of the true derailment rates to the extent permitted by the input data. It is
 425 observed that any region with low risk indicators, e.g. the number of turnouts and freight traffic
 426 density, can be investigated with one of the suggested assumptions; namely A-1 to 4 (see
 427 Section 4.2.2).
 428
- 429 • From the perspective of the regions with high-risk indicators, e.g. Kansas, some of the
 430 assumptions, particularly those, which relied on turnout counts, are observed to deviate from
 431 the observations. In contrast to wanting a larger sample size in the first bullet, the larger sample
 432 sizes in the assumptions in this case generally lead to decreasing precision when estimating
 433 derailment rates. In other words, the decrease in precision for larger sample sizes is largely
 434 associated with minimal or even non-existent data. This might arise mainly from the presence
 435 of errors in the assumptions or a strong dependence in the real data. It could also be the result
 436 of better statistical results following a heavily-tailed (asymmetrical) distribution in such
 437 situations.
 438
- 439 • From the perspective of assumption types, it can be identified that the assumptions regarding
 440 turnout counts are a weak spot even when being generated mathematically on the basis of a
 441 concrete belief. This study employs the proportion of turnout counts and rail-network length.
 442 As the EU countries are relatively more populated in comparison to the US, European rail
 443 networks thereby require a larger number of turnouts in a short rail section. In case of a paucity
 444 of reliable guidance on the estimation of the number of derailments in a given region,
 445 particularly with high exposure, the subjective judgment of an expert might be utilized before
 446 conducting the analyses. In order words, the study accepts that there is one turnout per 1.18
 447 miles in this region of the US, even though this suggestion reflects a much higher number of
 448 turnouts than the US has. Moreover, demand for rail service stems from demands elsewhere in
 449 the economy for the products that railways haul. That is, each state has unique characteristics,
 450 which cause each one to build more or less of a rail network. Therefore, unique turnout numbers
 451 for such regions are needed, found using real data or an expert's judgment, to reach the
 452 saturation of the sample.
 453

454 7 CONCLUDING REMARKS

455 To ensure a proper rail operation and achieve effectively safety goals, prevention of turnout-related
 456 derailment has been a topic of concern to railway operators and the general public. Derailment
 457 predictions for turnouts are typically obtained through highly complicated statistical analyses
 458 associated with large potential risks. In recent decades, increasing awareness in safety risk analysis and
 459 the management of rail networks has resulted in the necessity of calculating derailment probabilities,
 460 considering root causes, and determining which particular rail infrastructures are more or less exposed.

¹²Illinois has actually quite high risk indicators. However, the area covered by Illinois in the chosen region is identified as posing a derailment risk lower which is lower than that of the entire state.

461 This study focuses on component failure-related derailment at RTs. Considering the potential impact
 462 of climate on component failures, the study employs a large enough region in the US to investigate
 463 derailments without having to consider climatic variations.

464 The number of new suggestions for prediction of train derailment at RTs is presented in this paper.
 465 Based on engineering assumptions and observations, it can be identified that regions with a moderate
 466 occurrence of derailment rate yield congruent results regardless of whether the data resource is based
 467 on rational assumptions or real data. Also, the most vulnerable assumption is determined to be turnout
 468 counts. Subject-matter expert judgement is suggested for the integration of an such assumption in
 469 future failure analysis in railway engineering as well as in other congruent railway infrastructures.

470 The success of the land segmentation, on the other hand, can be underlined. The impact of climate on
 471 rail infrastructure failures is a well-known phenomenon. As this study segmented land area by state, a
 472 well-performing methodological structure is established, enabling the climate impact to be eliminated.
 473 The suggested methodology for derailment estimates is observed to have the ability to overcome the
 474 complexity of the prediction of derailment in the segmented region.

475 **8 ACKNOWLEDGEMENT**

476 The authors would like to thank British Department for Transport (DfT) for Transport - Technology
 477 Research Innovations Grant Scheme, Project No. RCS15/0233; and the BRIDGE Grant (provided by
 478 University of Birmingham and the University of Illinois at Urbana Champaign). The first author
 479 gratefully acknowledges Turkish Ministry of Education for supporting his PhD at University of
 480 Birmingham. The authors are sincerely grateful to the European Commission for the financial
 481 sponsorship of the H2020-RISE Project No. 691135 “RISEN: Rail Infrastructure Systems Engineering
 482 Network”, which enables a global research network that tackles the grand challenge of railway
 483 infrastructure resilience and advanced sensing in extreme environments (www.risen2rail.eu).

484 **9 Bibliography**

485 AAC, n.d. *Association of American Railroads*. [Online]
 486 Available at: <https://www.aar.org/data-center/railroads-states/>
 487 [Accessed 12 01 2018].

488 Albert, J., 1988. Computational Methods Using a Bayesian Hierarchical Generalized Linear Model.
 489 *Journal of the American Statistical Association* , 83(404), pp. 1037-1044.

490 Albert, J., 1996. A MCMC algorithm to fit a general exchangeable model. *Communications in Statistics*
 491 *- Simulation and Computation*, 25(3).

492 Albert, J. H., 1999. Criticism of a hierarchical model using Bayes factors. *Statistics in Medicine*, 18(3),
 493 pp. 287-305.

494 Anderson, R. & Barkan , C., 2004. Railroad Accident Rates for Use in Transportation Risk Analysis.
 495 *Transportation Research Record: Journal of the Transportation Research Board*, Volume 1863, pp.
 496 88-98.

497 Dindar, S. & Kaewunruen, S., 2017. Assessment of Turnout-Related Derailments by Various Causes.
 498 In: J. G. Pombo J., ed. *Recent Developments in Railway Track and Transportation Engineering*. Cham:
 499 Springer, pp. 27-39.

- 500 Dindar, S., Kaewunruen, S. & An, M., 2016. Identification of appropriate risk analysis techniques for
501 railway turnout systems. *Journal of Risk Research*.
- 502 Dindar, S., Kaewunruen, S. & An, M., 2017. Derailment-based Fault Tree Analysis on Risk
503 Management of Railway Turnout Systems. *Materials Science and Engineering*, 245(4).
- 504 Dindar, S., Kaewunruen, S. & An, M., 2019. A Bayesian-based hierarchical model for analysis of
505 climate on hazardous rail component failures.
- 506 Dindar, S., Kaewunruen, S., An, M. & Barrera, Á.-G., 2017. *Derailment-based Fault Tree Analysis on*
507 *Risk Management of Railway Turnout Systems*. Prague, s.n.
- 508 Dindar, S., Kaewunruen, S., An, M. & Osman, M., 2016. Natural hazard risks on railway turnout
509 systems. *Procedia engineering*, Volume 161, pp. 1254-1259.
- 510 Dindar, S., Kaewunruen, S., An, M. & Sussman, J., 2017. Bayesian Network-based probability analysis
511 of train derailments caused by various extreme weather patterns on railway turnouts. *Safety Science*,
512 Issue In Press.
- 513 Dindar, S., Kaewunruen, S. & Osman, M. H., 2017. *Review On Feasibility of Using Satellite Imaging*
514 *for Risk Management of Derailment Related Turnout Component Failures*. Prague, IOP Conf. Series:
515 *Materials Science and Engineering*, p. 245.
- 516 Dindar, S., Kaewunruen, S. & Osman, M. H., 2017. Review On Feasibility of Using Satellite Imaging
517 for Risk Management of Derailment Related Turnout Component Failures. *IOP Conference Series:*
518 *Materials Science and Engineering*, 245(4).
- 519 Dindar, S., Kaewunruen, S. & Sussman, J. M., 2017. Climate Change Adaptation for GeoRisks
520 Mitigation of Railway Turnout Systems. *Procedia engineering*, Volume 189, pp. 199-206.
- 521 Dindar, S., Under review. Hierarchical Modelling of Derailment-causing Component Failures for
522 Railway Turnouts: An Inverse Gamma-Poisson based Bayesian Prediction..
- 523 Gelman, A., 2006. *Prior distributions for variance parameters in hierarchical models*. Volume 1,
524 Number 3, pp. 515–533: *Bayesian Analysis*.
- 525 Glickman, T. S., Erkut, E. & Zschockec, M. S., 2007. The cost and risk impacts of rerouting railroad
526 shipments of hazardous materials. *Accident Analysis & Prevention*, 5(39), pp. 1015-1025.
- 527 Gustafson, P., Hossain, S. & Macnab, Y., 2003. Conservative prior distributions for variance
528 parameters in hierarchical models. *The Canadian Journal of Statistics*, Volume 31.
- 529 Ishak, M. F., Dindar, S. & Kaewunruen, S., 2016. *Safety-based maintenance for geometry restoration*
530 *of railway turnout systems in various operational environments*. Songkhla, Thailand, s.n.
- 531 Kawprasert, A. & Barkan, C., 2010. Communication and Interpretation of Results of Route Risk
532 Analyses of Hazardous Materials Transportation by Railroad. *Transportation Research Record:*
533 *Journal of the Transportation Research Board*.
- 534 Liu, X., 2017. Optimizing rail defect inspection frequency to reduce the risk of hazardous materials
535 transportation by rail. *Journal of Loss Prevention in the Process Industries*, Volume 48, pp. 151-161.

- 536 Nayak, P. R., Rosenfield, D. B. & Hagopian, J. H., 1983. *Event probabilities and impact zones for*
537 *hazardous materials accidents on railroads*, Washington D.C: U.S. Department of Transportation.
- 538 Sa'adin, S. L. B., Kaewunruen, S., Jaroszweski, D. & Dindar, S., 2016. *Operational risks of Malaysia-*
539 *Singapore high speed rail infrastructure to extreme climate conditions*. ART-2016, Jeju, Korea, The
540 1st Asian Conference on Railway Infrastructure and Transportation.
- 541 Treichel, T. T. & Barkan, C. P., 1993. *Working Paper on Mainline Freight Train Accident Rates*,
542 Washington, D.C: Research and Test Department, Association of American Railroads.
- 543 Xiang , L., Barkan, C. & Rapik, S. M., 2011. Analysis of Derailments by Accident Cause Evaluating
544 Railroad Track Upgrades to Reduce Transportation Risk. *Transportation Research Record*, Issue 2261,
545 pp. 178-185.
- 546 Xiang , L., Saat , R. M. & Barkan, C. . . P., 2017. Freight-train derailment rates for railroad safety and
547 risk analysis. *Accident Analysis and Prevention*, Issue 98, pp. 1-9.
- 548
- 549